ISBN: 978-3-95450-227-1 ISSN: 2673-5490 doi:10.18429/JACoW-IPAC2022-MOPOTK026

4-DIMENSIONAL EMITTANCE MEASUREMENTS AND CORRECTION OF UED OPTICS UP TO SEXTUPOLE ORDER*

W. H. Li[1], M. Gordon[2], M.B. Andorf[1], A. C. Bartnik[1], C. J. R. Duncan[1], M. Kaemingk[1], S. J. Levenson[1], C. A. Pennington[1], I. V. Bazarov[1], Y.-K. Kim[2], J. M. Maxson[1]
[1]Cornell Laboratory for Accelerator-Based Sciences and Engineering, Ithaca, NY 14853, USA
[2]University of Chicago Department of Physics, Chicago, IL 60637, USA

Abstract

Ultrafast electron diffraction imposes stringent constraints on the full 6D brightness of the probe electron beam. The desired normalized emittance, often in the few-nanometer regime and below, renders the beam very sensitive to field aberrations and space charge effects. In this proceeding, we report the correction of normal quadrupole, skew quadrupole, and sextupole aberrations in the MEDUSA ultrafast electron micro-diffraction beamline and measurements of the subsequent emittance. This low emittance is enabled by alkali-antimonide photocathodes driven at the photoemission threshold. We demonstrate that the measured emittance is consistent with that of optimized simulations with these cathodes, indicating that low emittance beams from high quality photocathodes can be preserved and used in practical applications.

INTRODUCTION

Ultrafast electron diffraction(UED), ultrafast electron microscopy (UEM), and X-ray free electron lasers are some of the most important modern tools for the study of non-equilibrium processes in crystals on the picosecond scale and below [1–11]. The spatial and temporal resolution of these devices is determined by the electron beam quality.

For UED in particular, the relevant metrics, the probe beam size and divergence, can be collectively represented in the emittance. The emittance of the electron beam can be degraded in transport by non-linear fields coming from space charge and electron optics, as well as stray fields from electron optics[12]. Correcting these stray fields is common up to quadrupole fields in photoinjectors [13–15]. As beam emittance is pushed ever smaller, emittance contributions from stray fields will matter increasingly more, and unless corrected, can become the dominant contribution to the final emittance of the beam. The effects of non-linear fields are especially important for beams with larger size, as the emittance contribution grows super-linearly with the beam size.

We have implemented stray field correction of quadrupole, skew quadrupole, and sextupole moments in order to preserve the emittance in MEDUSA, a keV UED microdiffraction beamline described in [16]. A schematic of the main elements of the beamline are shown in Fig. 1.

* This work was supported by the U.S Department of Energy, grant DE-SC0020144 and U.S. National Science Foundation Grant PHY-1549132, the Center for Bright Beams.

PHASE SPACE RECONSTRUCTION

We can characterize the quality of the beam by reconstructing the beam in the 4d phase space defined by x, x', y, and y'. This reconstruction is performed by scanning the electron beam across a 10 µm aperture placed at the sample location. The x and y coordinates are determined by the beam position on the aperture. The beam is then imaged on a downstream screen. With a sufficiently large distance between the aperture and screen and a small aperture, the distribution of the beam on the screen is dominated by the momentum at the aperture, not the position. Thus, the x' and y' distribution is determined by the distribution of the beam on the final screen.

Each pixel on the final screen at a particular aperture position, therefore, corresponds to a 4d "voxel" in 4d phase space. We can build up the 4d volume voxel by voxel by scanning the beam on the aperture and measuring the intensity at each pixel, which produces a full 4d phase space. Example 2d projections of the 4d measurement in a stray field corrected beam are shown in Fig. 2.

With the phase space in hand, we can calculate the 4d sigma matrix, defined as:

$$\Sigma_{4d} = \begin{pmatrix} < x^2 > & < xx' > & < xy > & < xy' > \\ < x'x > & < x'^2 > & < x'y > & < x'y' > \\ < yx > & < yx' > & < y^2 > & < yy' > \\ < y'x > & < y'x' > & < y'y > & < y'^2 > \end{pmatrix}. \quad (1)$$

We can quantify the preservation of beam quality by calculating the normalized 4d emittance, defined as:

$$\varepsilon_{n,4d} = (\beta\gamma)^2\sqrt{\det(\Sigma_{4d})}. \quad (2)$$

To more easily compare the 4d emittance with the 2d emittance, for the rest of this paper, the square root of the 4d emittance will be reported.

QUADRUPOLE CORRECTION

One important benefit of measuring the entire 4d phase space and calculating the 4d emittance lies in the ability to measure x-y correlations. These x-y correlations can be used to reveal the presence of stray quadrupole fields along the beamline. Such stray quadrupoles commonly require corrections in photoinjectors, as the induced skew correlations can significantly degrade the 2d emittance.

Large quadrupole moments can be most easily seen in the beam size and shape. Figure 3 (a) shows the beam size as a function of solenoid current, and there is a clear asymmetry

ISBN: 978-3-95450-227-1 ISSN: 2673-5490 doi:10.18429/JACoW-IPAC2022-MOPOTK026

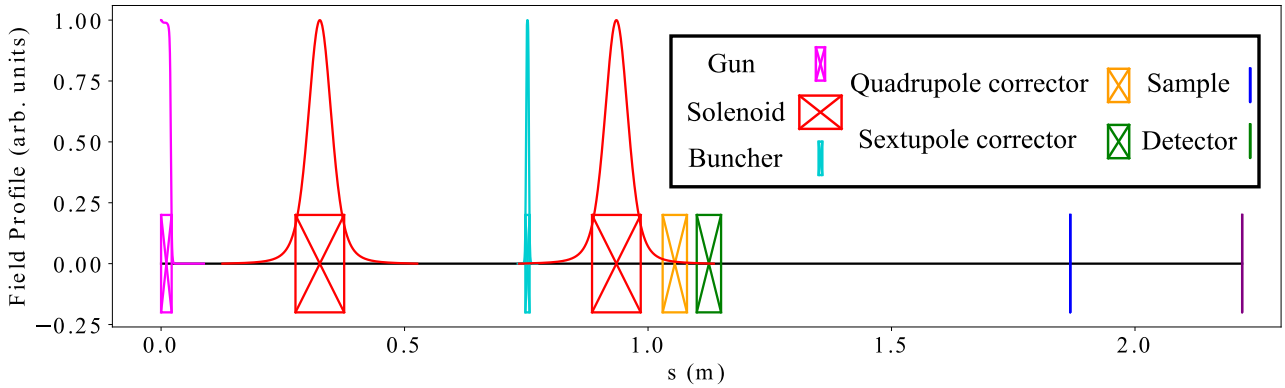

Figure 1: A schematic of the relevant elements of the MEDUSA ultrafast electron diffraction beamline. The locations of each element are shown by the boxes, with their field profiles overlaid on top. For the measurements described in this proceeding, an aperture was placed at the sample location.

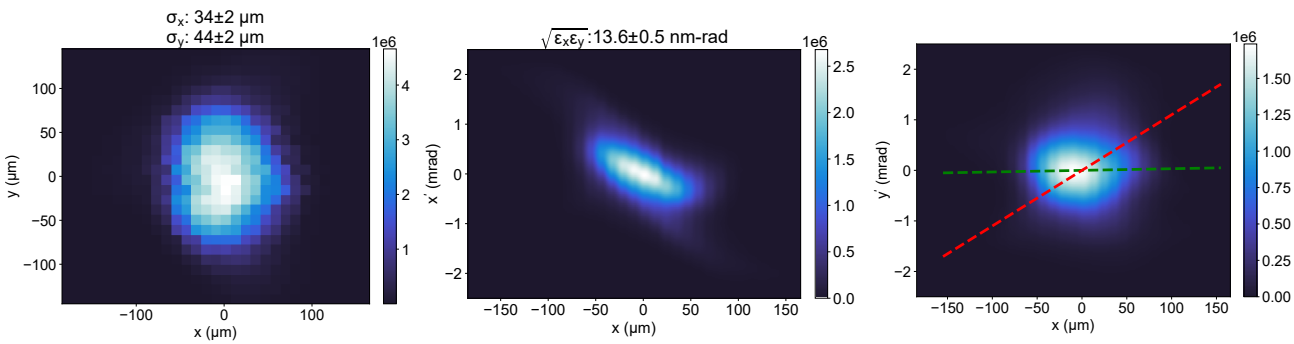

Figure 2: From left to right, $x-y$, $x-x'$, and $x-y'$ projections of the reconstructed 4d density matrix at the sample location with stray field correction. The dashed green line in (b) shows the correlation between x and y' which is seen to be near 0 compared to the red line, which represents the correlation before correction.

in the x and y beam sizes. We model the stray fields as normally oriented quadrupoles inside both of the solenoids. Using General Particle Tracer (GPT), a particle-in-cell particle tracker, we are able to fit for the quadrupole strengths, and the simulated solenoid scan agrees well with the measured data.

As further confirmation of the correctness of the model, Fig. 3 (b) shows the skew angle of the beam as a function of solenoid current. We use skew angle as a proxy for the beam shape, as it shows the direction that the beam is stretched in. The blue arrows on the plot provide a visual representation of the directions indicated by the skew angles. The inset shows an example of a beam with an obvious skew, and the blue arrow shows the skew direction. The same quadrupole strengths fit the skew angle extremely well.

We can simulate the effects of the uncorrected stray quadrupole moments on two figures of merit that are particularly relevant for ultrafast electron diffraction experiments. These are the incident charge on the sample and the emittance. The incident charge is affected by the quadrupoles since we use a probe-defining aperture immediately before the sample to perform diffraction on micron-scale samples. The charge on target is thus set by the beam size on the aperture. The emittance has both a direct effect on transmission and the momentum-space resolution of the probe. At the fitted values of the quadrupole moments, we find that the emittance has increased by roughly a factor of 4 from the zero-quad baseline, while the transmission has fallen by nearly a factor of 20.

In [17], an analytic treatment of stray quadrupole moments in photoinjectors has shown that the large adverse effects of these moments can be avoided with tunable quadrupole corrector magnets. The locations of these quadrupole correctors need not match the locations of the stray quads; in fact, the only requirement is that the correctors be located where the beam is large. We implement this solution by placing both a normal and a skew quadrupole corrector immediately after the second solenoid. As can be seen in Fig. 2, we are able to remove x-py correlations, and thus, correct the stray quadrupole moments.

SEXTUPOLE CORRECTION

A sextupole moment is present in the beamline, which is known because of the triangular shape of the beam on the final detector. To fix this sextupole, the downstream sextupole corrector is rotated to produce a sextupole moment

ISBN: 978-3-95450-227-1 ISSN: 2673-5490 doi:10.18429/JACoW-IPAC2022-MOPOTK026

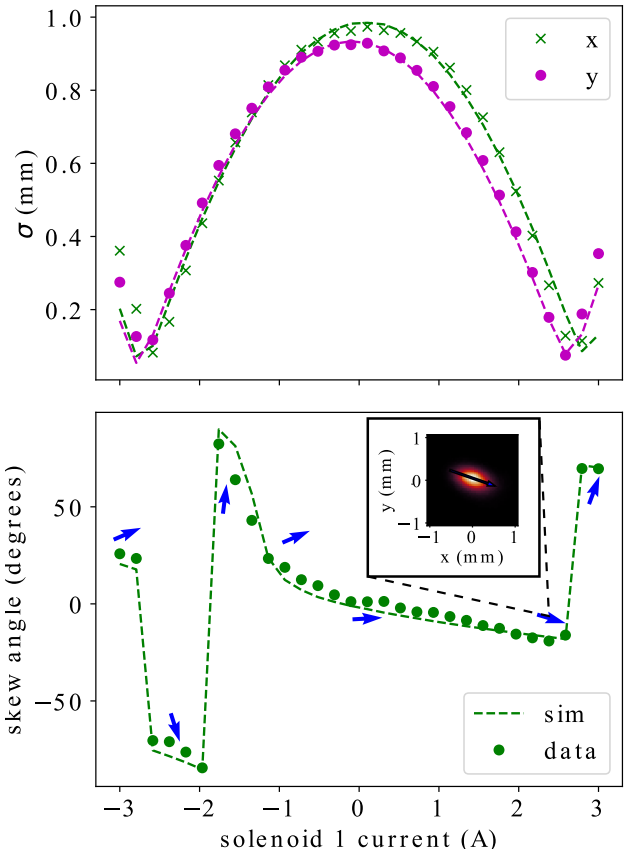

Figure 3: Experimental data showing the presence of a quadrupole moment in the (a) beam size and (b) beam shape. We use the skew angle (inset) as a measurement of beam shape, and the arrows provide a visualization of several representative angles. Dashed lines show a simulated solenoid scan performed in GPT and show good agreement with the experimental data.

which is anti-aligned with the applied field, up to the rotation induced by the solenoid. The current is then adjusted in the corrector to find the optimal cancellation.

The beam size and emittance for different buncher voltages around the operating voltage both with and without the sextupole corrector are shown in Figs. 4a and 4b. The curves on the graphs represent simulations done in GPT. The shape of the curves is dependent on the MTE of the initial beam. The best fit for the beam size and emittance plots uses a MTE of 70 meV. The red curve was created assuming no stray fields in the beamline. The blue curve was created by placing a sextupole in the buncher and adjusting the strength of the sextupole.

CONCLUSION

As photoinjectors push for smaller intrinsic emittance, aberrations which have previously been ignored have increasingly significant impacts on the downstream emittance of the electron beam. Preserving the quality of these beams from production to application requires the cancellation of higher order stray moments in the beamline. By designing

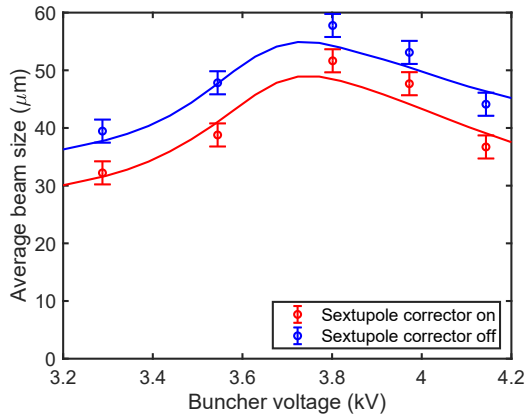

(a)

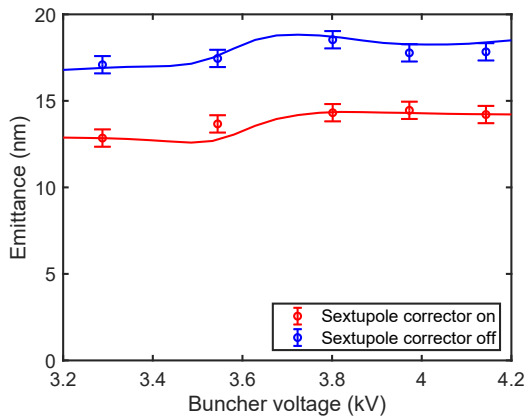

(b)

Figure 4: (a) Beam size and (b) transverse normalized rms emittance at different buncher voltages. Lines represent GPT simulations with a MTE of 70 MTE. The red lines assume no stray fields in the beamline. The blue lines were created assuming a sextupole stray field in the buncher with no correction.

and tuning magnets up to sextupole, the effects of these stray moments on a UED beamline were corrected, and the emittance of the beam is well predicted by simulation.

ACKNOWLEDGEMENTS

This work was supported by the U.S Department of Energy, grant DE-SC0020144 and U.S. National Science Foundation Grant PHY-1549132, the Center for Bright Beams.

REFERENCES

[1] A. H. Zewail, "4d ultrafast electron diffraction, crystallography, and microscopy," *Annual Review of Physical Chemistry*, vol. 57, no. 1, pp. 65–103, 2006, doi:10.1146/annurev.physchem.57.032905.104748

[2] X. Wang, D. Xiang, T. Kim, and H. Ihee, "Potential of femtosecond electron diffraction using near-relativistic electrons from a photocathode rf electron gun," *Journal-Korean Physical Society*, vol. 48, no. 3, p. 390, 2006.

ISBN: 978-3-95450-227-1 ISSN: 2673-5490 doi:10.18429/JACoW-IPAC2022-MOPOTK026

[3] S. P. Weathersby, G. Brown, M. Centurion, T. F. Chase, *et al.*, "Mega-electron-volt ultrafast electron diffraction at slac national accelerator laboratory," *Review of Scientific Instruments*, vol. 86, no. 7, p. 073 702, 2015, doi:10.1063/1.4926994

[4] M. Gao *et al.*, "Mapping molecular motions leading to charge delocalization with ultrabright electrons," *Nature*, vol. 496, no. 7445, pp. 343–346, 2013.

[5] S. Wall *et al.*, "Atomistic picture of charge density wave formation at surfaces," *Physical Review Letters*, vol. 109, no. 18, p. 186 101, 2012.

[6] M. Eichberger *et al.*, "Snapshots of cooperative atomic motions in the optical suppression of charge density waves," *Nature*, vol. 468, no. 7325, pp. 799–802, 2010.

[7] P. Emma *et al.*, "First lasing and operation of an ångstrom-wavelength free-electron laser," *Nature Photonics*, vol. 4, no. 9, pp. 641–647, 2010.

[8] B. W. J. McNeil and N. R. Thompson, "X-ray free-electron lasers," *Nature Photonics*, vol. 4, no. 12, pp. 814–821, 2010, doi:10.1038/nphoton.2010.239

[9] T. Ishikawa *et al.*, "A compact x-ray free-electron laser emitting in the sub-ångström region," *nature photonics*, vol. 6, no. 8, pp. 540–544, 2012.

[10] Ding *et al.*, "Measurements and simulations of ultralow emittance and ultrashort electron beams in the linac coherent light source," *Phys. Rev. Lett.*, vol. 102, p. 254 801, 25 2009, doi:10.1103/PhysRevLett.102.254801

[11] M. Altarelli *et al.*, *XFEL: The European X-Ray Free-Electron Laser. Technical design report*, 2006, doi:10.3204/DESY_06-097

[12] D. Dowell, "Sources of emittance in rf photocathode injectors: Intrinsic emittance, space charge forces due to non-uniformities, rf and solenoid effects," *Cornell U physics ArXive*, 2016, doi:10.48550/arXiv.1610.01242

[13] A. Bartnik, C. Gulliford, I. Bazarov, L. Cultera, and B. Dunham, "Operational experience with nanocoulomb bunch charges in the Cornell photoinjector," *Phys. Rev. ST Accel. Beams*, vol. 18, no. 8, p. 083 401, 2015, doi:10.1103/PhysRevSTAB.18.083401

[14] D. Dowell *et al.*, "The development of the linac coherent light source rf gun," *ICFA Beam Dynamics Newsletter No. 46*, vol. 46, p. 162, 2008.

[15] L. Zheng *et al.*, "Experimental demonstration of the correction of coupled-transverse-dynamics aberration in an rf photoinjector," *Phys. Rev. Accel. Beams*, vol. 22, no. 7, p. 072 805, 2019, doi:10.1103/PhysRevAccelBeams.22.072805

[16] W. H. Li *et al.*, "A kiloelectron-volt ultrafast electron microdiffraction apparatus using low emittance semiconductor photocathodes," *Structural Dynamics*, vol. 9, no. 2, p. 024 302, 2022, doi:10.1063/4.0000138

[17] D. H. Dowell, F. Zhou, and J. Schmerge, "Exact cancellation of emittance growth due to coupled transverse dynamics in solenoids and rf couplers," *Phys. Rev. Accel. Beams*, vol. 21, no. 1, p. 010 101, 2018, doi:10.1103/PhysRevAccelBeams.21.010101